arXiv:astro-ph/0002182v1 8 Feb 2000

INFNFE-02-00

Stellar Evolution and Large Extra Dimensions

S. Cassisi [1], V. Castellani [2], S. Degl'Innocenti [2], G. Fiorentini [3] and B. Ricci [3]
[1] *Osservatorio Astronomico di Collurania, via Maggini10, I-64100 Teramo, Italy.*
[2] *Dipartimento di Fisica dell'Università di Pisa and Istituto Nazionale di Fisica Nucleare, Sezione di Pisa, via Livornese 582/A, S. Piero a Grado, 56100 Pisa.*
[3] *Dipartimento di Fisica dell'Università di Ferrara and Istituto Nazionale di Fisica Nucleare, Sezione di Ferrara, via Paradiso 12, I-44100 Ferrara, Italy .*
(February 2000)

Abstract

We discuss in detail the information on large extra dimensions which can be derived in the framework of stellar evolution theory and observation. The main effect of large extra dimensions arises from the production of the Kaluza-Klein (KK) excitations of the graviton. The KK-graviton and matter interactions are of gravitational strength, so the KK states never become thermalized and always freely escape. In this paper we first pay attention to the sun. Production of KK gravitons is incompatible with helioseismic constraints unless the $4+n$ dimensional Planck mass M_s exceeds 300 Gev/c^2. Next we show that stellar structures in their advanced phase of H burning evolution put much more severe constraints, $M_s > 3-4$ TeV/c^2, improving on current laboratory lower limits.

I. INTRODUCTION

Recently there has been a revived interest in the physics of extra-spatial dimensions. In order to provide a framework of solving the hierarchy problem, in refs. [1–3], the fundamental Planck scale - where gravity becomes comparable in strength with the other interactions - was taken to be near the weak scale. The observed weakness of gravity at long distances is due to the presence of n new spatial dimensions, with size R which are large compared to the electroweak scale. The relation between the Planck mass in 4 dimensions ($M_{Pl} = \sqrt{\hbar c/G_N} = 1.2\,10^{19}$GeV/c^2) and that in $4+n$ dimensions (M_s) is

$$R^n = (\hbar/c)^n M_{Pl}^2/(M_s^{n+2}\,\Omega_n) \tag{1}$$

where Ω_n is the volume of the n-dimensional sphere with unit radius. Laboratory limits, essentially from LEP II [4] give a lower bound on M_s of about 1 TeV/c^2. The choice $M_s \sim 1$ TeV/c^2 yields $R \sim 10^{32/n-17}$ cm. The case $n = 1$ gives $R \simeq 10^{15}$cm which is excluded

since it would modify newtonian gravitation at solar system distances. Already for $n = 2$ one has $R \simeq 1$mm which is the distance where our present experimental measurement of gravitational forces stops, and one needs information from different sources.

In this context, one should remind that in last decades the improved knowledge of several physical mechanisms has allowed astrophysicists to produce stellar models with a significant degree of reliability. As a matter of fact, current stellar models nicely reproduce the large variety of stellar structures populating the sky, passing also some subtle tests as the ones recently provided by seismologic investigations of our sun. Such a success has already opened the way of using stellar structures as a natural laboratory to test the space allowed for new physics, i.e., to investigate the allowed modifications of the current physical scenario [5]. This looks as a quite relevant opportunity, bearing in mind that a stellar structure is governed by the whole ensemble of physical laws investigated in terrestrial laboratories and that these stellar structures, in varying their mass and ages, experience a range of physical situations not yet reached in current laboratory experiments. On this basis, the "stellar laboratory" has already provided relevant constraints on several physical ingredient as, e.g., the existence of Weak Interacting Massive Particles [6,7] or the neutrino magnetic moments [8,9].

Astrophysical constraints on large extra dimensions have been discussed in [3] and in [10]. The main effect of large extra dimensions arises from the production of the Kaluza-Klein (KK) excitations of the graviton. The KK-graviton and matter interactions are of gravitational strength, so the KK states never become thermalized and always freely escape. The associated energy loss (through photon-photon annihilation, electron-positron annihilation, gravi-Compton-Primakoff scattering, gravi-bremsstrahlung, nucleon-nucleon bremsstrahlung) have been calculated in [10] and observational constraints on M_s have been derived from simple considerations on the energetics of sun, red giants and supernovae.

In this paper we discuss in more detail the information on large extra dimensions which can be derived in the framework of stellar evolution theory and observation. The first part is devoted to the study of the sun, which represents a privileged laboratory in view of the richness and accuracy of available data. In particular we shall consider the following topics:
i)As well known there is a remarkable agreement between the predictions of the Standard Solar Model (SSM) and the results of helioseismic observations, see e.g. [11–13]. Production of KK gravitons provides a new energy loss, which will become incompatible with helioseismic constraints if the $4 + n$ dimensional Planck mass M_s is sufficiently low. In this way we shall determine lower limits on M_s from helioseismic observations.
ii)Despite its several successes, the standard solar model presents us with some puzzles, e.g. the deficit of solar neutrinos, see e.g. [14], the depletion of the photospheric lithium abundance, see e.g. [15], and - perhaps - an underestimate of the sound speed just below the convective envelope, see e.g. [12,16]. Could it be that the new physics of KK-graviton production accounts for some of these anomalies?

In addition, the efficiency of KK-graviton energy loss appears strongly dependent on the temperature. This suggests to consider stars experiencing internal temperatures much larger than in the sun and which, in turn, are particularly sensitive to the efficiency of cooling mechanisms. In this way the investigation will be extended to red giants structures, which will provide a much more stringent limit on M_s.

In section II we give a first look at KK-graviton production in the sun, determining the order of magnitude of the acceptable M_s and presenting the structure of solar models where

the new energy loss is relevant. In section III we shall determine the helioseismic constraints on M_s, from data on the photospheric helium abundance and on sound speed in the energy production region. The effect of KK-graviton production on the "solar puzzles" mentioned above is discussed in sect. IV. Sect. V will be devoted to red giant stars.

Our conclusions are summarized at the end of the paper, whereas in the appendix we collect the relevant formulas for the energy losses.

II. A FIRST LOOK AT THE EFFECTS OF KK-GRAVITON PRODUCTION IN THE SUN

It is interesting to compare the energy loss due to KK-graviton production with the energy production from the pp chain at the center of the sun. The values of density, temperature and chemical composition derived from the SSM of [16] are presented in Table I. The results of other SSM calculations are similar, see e.g. [17]. Energy loss and production rates, computed according to the results of Appendix A, are compared in Table II. The most important contribution always comes from the photon-photon annihilation.

One expects that the solar solar structure would be drastically modified if the energy loss due to KK-gravitons becomes comparable with the nuclear energy production rate. In this way one can derive the following lower limits on M_s:

$$n = 2 : \quad M_s > 140\, GeV/c^2 \tag{2}$$

$$n = 3 : \quad M_s > 3.5\, GeV/c^2 \tag{3}$$

This result which is essentially the same as that in ref. [10] suggests that we concentrate on the $n = 2$ case only. So far we assumed just a rough knowledge of the solar structure. One can expect that more detailed information, as that provided by helioseismology, provide more stringent constraints.

To understand in more detail the effect of KK-graviton production we have built solar models which include this additional energy loss. The energy generation subroutine was modified so as to include the KK-graviton loss and the stellar evolution code FRANEC [18] was run by varying the three free parameters of the model (initial helium abundance Y_{in}, initial metal abundance Z_{in} and mixing length α) until it provides a solar structure (i.e. it reproduces the observed solar luminosity, radius and photospheric metal abundance at the solar age).

As an example, we present here the case $M_s = 0.2$ TeV/c^2. The main differences with respect to our SSM are depicted in Table III and Fig. 1. Several features can be easily understood by observing that the solar model with KK-graviton production has to produce, now and in the past, a higher amount of nuclear energy, in order to compensate for the additional energy loss.

More hydrogen has been burnt into helium, and the initial helium abundance has to be reduced with respect to the SSM (otherwise one would get a stellar structure which, being too much helium rich, would be presently overluminous). Consequently, the present photospheric helium abundance Y_{ph} is decreased with respect to the SSM prediction.

Nevertheless, the central helium abundance is still somehow larger than in SSM and more energy is being produced in order to compensate for the KK-graviton losses. This is achieved with a somehow larger central temperature.

In the solar core, both temperature and "mean molecular weight" are thus higher than in the SSM, so that one cannot a priori decide for the behaviour of the sound speed. In fact Fig. 1 shows a decrease near the center and a significant increase near $R = 0.2R_{\odot}$, i.e. in a region where helioseismic determinations are still very accurate.

These observations will be useful for determining the relevant observables which are sensitive to M_s and which can be constrained by means of helioseismology.

In Fig. 2 we also compare the nuclear energy production rate with the losses due to KK-gravitons. The results are consistent with the qualitative energetics analysis discussed above.

III. HELIOSEISMIC CONSTRAINTS ON M_S

Helioseismology provides detailed information on several solar properties. In particular, the sound speed profile and the photospheric helium abundance Y_{ph} are determined with high accuracy. In ref. [11] it was estimated that the isothermal sound speed squared, $u = P/\rho$ at distance $R = 0.2R_{\odot}$ is determined with an accuracy of about $\Delta u/u \approx 1 \cdot 10^{-3}$,

$$u_{0.2}^{\odot} = (1.238 \pm 0.001) \cdot 10^{15}\, cm^2/s^2 \tag{4}$$

This uncertainty, defined as the "statistical" [11] or "one sigma" error [14], was obtained by taking into account all possible contributions arising from: i) measurement errors, ii) the inversion method and iii) the choice of the reference model (the recent analysis of [13] confirms the estimate of [11] for each contribution to the uncertainty). These estimated errors were added in quadrature. With a similar attitude the uncertainty of Y_{ph} was estimated:

$$Y_{ph}^{\odot} = 0.249 \pm 0.003 \tag{5}$$

Recent accurate standard solar model calculations are successful in reproducing sound speed in the energy production region as well as the photospheric helium abundance, their predictions being quite close to the central helioseismic estimates, see e.g. [16,11]. On the other hand, as discussed in the previous section, both quantities are sensitive to the energy loss due to KK-graviton production For this reason, we concentrate here on Y_{ph} and on the value of u at $R = 0.2R_{\odot}$ hereafter $u_{0.2}$.

We have built a series of solar models with M_s in the range of few hundred GeV/c^2 in order to determine the dependence of both observables on M_s, see Figs. 3 and 4. For each observable Q the results have been parametrized in the form

$$Q(M_s) = Q_{SSM}(1 + (m/M_s)^{\alpha}) \quad , \tag{6}$$

with the results for the parameters m and α shown in Table IV. By requiring that the differences in the calculated observables do not exceed the helioseismic uncertainty, we get the following lower bounds on M_s:

-from Y_{ph} : $M_s > 0.23$ TeV/c^2

-from $u_{0.2}$: $M_s > 0.31$ TeV/c^2

These bounds are stronger that that of Eq. (2), which was obtained by using crude energetical considerations. However, the accuracy of helioseismic method has yielded an improvement of just a factor of two. In fact, KK-graviton energy loss rate ϵ_{KK} depends on high powers of M_s, so that drastic changements of ϵ_{KK} result from just tiny modifications of M_s.

IV. EXTRA-DIMENSIONS AND THE PUZZLES OF THE SSM

As well known, in front of its several successes, the standard solar model presents us with some puzzles:
i) The signals measured by all solar neutrinos experiments are systematically lower than those predicted by SSMs, an effect which is now commonly ascribed to neutrino oscillations.
ii) The observed photospheric lithium abundance is a factor of hundred smaller than the meteoritic value [15]. Lithium is being continuosly mixed in the convective envelope, however -according to the SSM - it should not be destroyed by nuclear reactions since even at the bottom of the convective zone the temperature is not high enough to burn it. This signals some deficiency of the standard solar model, which is built in a one dimensional approximation and neglects rotation, see [19].
iii) The helioseismically determined sound speed just below the convective envelope is somehow smaller (by 0.4%) with respect to the predictions of the most recent and accurate SSM calculations, see e.g. [12,16].

It is thus natural to ask what is the effect of the hypothetical large extra dimensions on these items. [1]

Concerning solar neutrinos, the answer is already contained in the previous discussion. When KK-graviton production is effective, the central temperature increases and consequently the production of Beryllium and Boron neutrinos is increased, see Table III. KK-graviton production would thus make the neutrino puzzle even more serious. At the bottom of the convective zone the temperature would be even smaller than that predicted by SSM, see Table III, so that there is no help in lithium burning. Sound speed just below the convective enevelope is practically unchanged with respect the SSM, so that the disagreement cannot be affected.

In short, KK graviton production would provide no cure to the SSM puzzles.

---

[1] We recall that in [20] conversion of electron neutrinos to the light fermions propagating in the bulk of $4 + n$ dimensions has been considered as a solution of the solar neutrino problem.

V. RED GIANTS AND KK-GRAVITONS

A glance at the current evolutionary scenario easily indicates low-mass Red Giant Branch (RGB) stars as good candidates for investigating the effects of KK-graviton production. As a matter of fact a RGB star reaches internal temperatures of the order of 10^8 K. Moreover, the structure of RGB stars is quite sensitive to the cooling mechanisms which regulate the size of the He core at the He ignition. The size of He core in turn governs several observational quantities both in these RGB structures as well as in the subsequent phase of central He burning (Horizontal Branch, HB) stars. We will follow this approach discussing the effect of KK-graviton cooling on the evolution of suitable RGB structures. Comparison of theoretical predictions with available experimental (i.e. observational) data will allow to put more stringent constraints on the minimal $4+n$ dimensional Planck mass M_s.

To perform our investigation we used our latest version of the FRANEC evolutionary code [18] to predict the observational properties of stellar models with different metallicities but with a common age of the order of 10 Gyr, thus adequate for RGB stars actually evolving in galactic globular stellar clusters (GCs). In order to make more clear to the reader the following discussion, in Fig. 5 we show the typical Hertzprung-Russel diagram for a galactic GC (upper panel) and the corresponding theoretical one (lower panel) as obtained by using the prescriptions provided by our own computations. The most relevant evolutionary phases and observational features are clearly marked. The diagram represents the locus of stars for a given chemical composition and age but different masses. As the mass increases, the star moves from the Main Sequence location (H central burning phase) to the RGB (H shell burning phase) till reaching a maximum luminosity where the central He ignition occurs (RGB tip), driving the structure to the central He burning (Horizontal Branch) phase.

Numerical experiments disclose that a stronger cooling has a little effect on the morphology of the diagram depicted in Fig. 5, but severe consequences on the internal structure of the star. Fig. 6 shows the predicted time dependence of the central temperature– density relation for selected values of M_s and $n = 2$. As expected, one finds that by increasing M_s the efficiency of the extra-cooling decreases. Above $M_s \simeq 5$ TeV/c^2 the effects on the evolutionary history of the stellar structure vanish. Even a quick inspection of data in Fig. 6 reveals that the assumption $M_s \sim 1.5$ TeV/c^2 (i.e. already above the current accelerator lower limit for M_s) is deeply affecting the structure so that one expects strong observational consequences. As a matter of fact, by exploring the case M_s=1 TeV/c^2 (the previous lower limit) one finds that RGB stars would fail to ignite Helium, running against the well-established evidence of Helium burning star in galactic GCs. Fig. 6 shows that increasing the cooling for each given central density the central temperature is lower, as expected. According to well known prescriptions of the stellar evolutionary theory, one can thus easily predict that the end of the RGB phase – i.e. the central He ignition – will be delayed and the mass of the He core at this stage will be larger.

To discuss this point in some detail, we show in Fig. 7 the He core mass at the central He ignition (RGB tip) for selected assumptions about the value of M_s and n=2. As shown in the same Fig. 7 in order to cover the range of metallicity (Z) spanned by the galactic GCs, computations have been performed for a $0.8M_\odot$ star with Z=0.0002 and for $1M_\odot$ star with Z=0.02.

To constrain the value of M_s one has now to discuss theoretical results in terms of

observable quantities. In this context one finds that the extra-cooling is governing two main observational parameters: i) the luminosity of the RGB tip, ii) the luminosity of He burning HB stars. In both cases the stronger the extra-cooling the larger is the predicted luminosity.

In this paper, we focus our attention on the first parameter only. Several papers have already remarked the good agreement between observations and standard model theoretical predictions [21,22]. Such good agreement is shown also in Fig. 8 where we report luminosity (in bolometric absolute magnitudes) of the brightest observed RGB star in clusters with different metallicities [24,25] as compared with theoretical predictions for the canonical scenario ($M_s \to \infty$). According to the discussions given in several papers (see e.g. [23,22]) the theoretical predictions should represent within about 0.1 mag. the *upper envelope* of the observed star luminosity, and this is precisely what one finds in Fig. 8. However, the same figure shows that for finite value of M_s theoretical predictions move toward larger luminosity, in disagreement with observations.

By inspection of data in Fig. 8 one can conclude conservatively that values of $Ms \leq 3$ TeV/c^2 are definitively ruled out by the observational tests, whereas a lower limit of 4 TeV/c^2 appears reasonably acceptable. Thus this detailed evolutionary investigation has improved the crude estimate of ref [10] $M_s \gtrsim 2$ TeV/c^2.

VI. CONCLUDING REMARKS

We summarize here the main points of this paper:

i)Helioseismic constraints on the sound speed in the energy production region and on the photospheric helium abundance rule out values of the $4+2$ dimensional Planck mass below $M_s = 0.3$ TeV/c^2.
ii)The introduction of additional energy loss due to KK-graviton production cannot be a cure to the puzzles posed by SSM calculations. In particular, the predicted neutrino signals would be even larger than those of the SSM.
iii)Observational constraints for Red Giant stars evolving in galactic globulars imply $M_s > 3-4$ TeV/c^2. This bound is stronger than that provided by accelerator, thus indicating how useful it is, and hopefully it will be, the synergetic use of terrestrial and stellar laboratories.

ACKNOWLEDGMENTS

We are extremely grateful to Z. Berezhiani, D. Comelli and F. Villante for discussions. This work is co-financed by the Ministero dell'Università e della Ricerca Scientifica e Tecnologica (MURST) within the "Astroparticle Physics" project.

APPENDIX A: STAR ENERGY-LOSS VIA KK-GRAVITONS

The energy loss rate per unit mass due to escaping KK gravitons has been calculated in [10]. Three processes are important for KK-graviton production in the sun and in the red giants. The relevant formulas are collected below, in natural units as well as in units

more useful for implementation in a stellar evolution code. For a comparison, the energy production rate per unit mass due to the pp-chain is also parametrized.

a. Photon photon annihilation to KK gravitons: $\gamma + \gamma \rightarrow grav$

When n extra dimensions are effective, the Newtonian interaction potential [$V \sim 1/(M_{pl}^2 r)$]is modified to $V \sim 1/(M_s^{n+2} r^{1+n})$, so that the coupling of each particle to the gravitational field is proportional to $1/M_s^{1+n/2}$ and KK-graviton production cross sections are proportional to the square of this quantity. A thermal photon gas is uniquely specified by its temperature T and fundamental physical constants ($\hbar, c$ and K_B) so that dimensional considerations fix the dependence of the energy loss rate per unit volume Q_γ. In natural units, this has dimension of [Energy]^5, so that one has $Q_\gamma = A_\gamma(n) M_s^{-n-2} T^{n+7}$ where $A_\gamma(n)$ are numerical coefficients given in eq. (7) of [10]. The energy loss rate per unit mass is obtained by dividing Q by the mass density ρ. When temperature is in expressed in Kelvin degress, density in g/cm^3 and M_s in TeV/c^2, the energy loss ϵ_γ in erg/g/s is thus:

$$n = 2 \quad \epsilon_\gamma = 7.25 \cdot 10^{-66} \frac{T^9}{\rho M_s^4} \tag{A1}$$

$$n = 3 \quad \epsilon_\gamma = 4.42 \cdot 10^{-82} \frac{T^{10}}{\rho M_s^5} \tag{A2}$$

b. Gravi-compton Primakoff scattering: $\gamma + e \rightarrow e + grav$

The expression for the energy loss is in this case:

$$\epsilon_{GCP} = B(n) \frac{\alpha}{m_e} \frac{n_e}{\rho} \frac{T^{n+5}}{M_s^{n+2}} \tag{A3}$$

where the numerical coefficients $B(n)$ are found in eq. 15 of [10], $m_e(n_e)$ is the electron mass (numerical density). The dependence on M_s is easily understood from the previous considerations, α comes in from electro-magnetic coupling of the electron and the factor n_e/ρ clearly expresses the proportionality to the electron number per unit mass. Dimensional analysis is not sufficient to fully specify the dependence on temperature due to the presence of another mass scale, m_e, which is relevant for non-relativistic electrons, see [3]. In the same units as in eq. (A1,A2):

$$n = 2 \quad \epsilon_{GCP} = 1.69 \cdot 10^{-78} \frac{T^7 n_e}{\rho M_s^4} \tag{A4}$$

$$n = 3 \quad \epsilon_{GCP} = 5.60 \cdot 10^{-94} \frac{T^8 n_e}{\rho M_s^5} \tag{A5}$$

c. Gravi-Bremsstrahlung: $e + Z \to e + Z + grav$

The energy loss is now:

$$\epsilon_{GB} = C(n)\alpha^2 \frac{n_e}{\rho} \frac{T^{n+1}}{M_s^{n+2}} \Sigma_j n_j Z_j^2 \tag{A6}$$

where n_j is the number density of nuclei with atomic number Z_j and the numerical factors $C(n)$ are given in eq. (21) of [10]. In the same units of eqs. (A1,A2) one has:

$$n = 2 : \quad \epsilon_{GB} = 5.86 \cdot 10^{-75} \frac{T^3 n_e}{\rho M_s^4} \Sigma_j n_j Z_j^2 \tag{A7}$$

$$n = 3 : \quad \epsilon_{GB} = 9.74 \cdot 10^{-91} \frac{T^4 n_e}{\rho M_s^5} \Sigma_j n_j Z_j^2 \tag{A8}$$

The total energy loss due to KK-graviton production is

$$\epsilon_{KK} = \epsilon_\gamma + \epsilon_{GCP} + \epsilon_{GB} \tag{A9}$$

It is useful to compare the above energy losses with the e.m. energy production rate per unit mass from the pp-chain. The slowest reaction of the chain is the $p + p \to d + e^+ + \nu_e$ which in the temperature region of interest for the sun, has a rate $< \sigma v >_{pp} = AT^{3.83}$, with $A = 4.398 \cdot 10^{-71}$ cm^3/s and T is expressed in Kelvin. The energy production rate per unit mass through the ppI termination of the pp-chain is:

$$\epsilon_{ppI} = \frac{1}{4} \rho \frac{X^2}{m_H^2} Q_{em} < \sigma v >_{pp} \tag{A10}$$

where $Q_{em} = 26.1$ MeV is the average e.m. energy released in the $4p + 2e^- \to^4 He + 2\nu_e$, X is the H-mass fraction and m_H is the hydrogen mass. In the same units as in Eq. (A1) one has:

$$\epsilon_{ppI} = 2.97 \cdot 10^{-27} X^2 \rho T^{3.83} \tag{A11}$$

As well known the ppI branch is the main energy source in the Sun. Everywhere it gives the strongest contribution to the energy production rate:

$$\epsilon_{nuc} = \epsilon_{ppI} + \epsilon_{ppII} + \epsilon_{ppIII} + \epsilon_{CNO} \, . \tag{A12}$$

REFERENCES

[1] N. Arkani-Hamed, S. Dimopoulos and G. Dvali, Phys. Lett. B 429 (1998) 263.

[2] I. Antoniadis, N. Arkani-Hamed, S. Dimopoulos and G. Dvali, Phys. Lett. B 436 (1998) 257.

[3] N. Arkani-Hamed, S. Dimopoulos and G. Dvali, Phys. Rev. D59 (1999) 086004.

[4] For a review see e.g. G.F. Giudice, hep-ph/9912279, to appear in the Proceeding of the XIX International Symposium on Lepton and Photon Interactions at High Energies, Stanford University, August 1999, http://lp99.slac.stanford.edu/; V. Ruhlmann-Kleider, ibidem.

[5] G. Raffelt, "Stars as laboratories for fundamental physics", The University Chicago Press, Chicago 1996.

[6] R. Rood and A.Renzini, Proc. 3rd ESO-Cern Symposium "Astronomy, Cosmology and Fundamental Physics", M.Caffo, R.Fanti, G.Giacomelli and A.Renzini eds., p.287. (1989)

[7] D.N. Spergel and J. Faulkner, Ap. J. Letter 331 (1988) 21

[8] G.Raffelt, Ap. J. 365 (1990) 559.

[9] V.Castellani and S.Degl'Innocenti, Ap. J. 402 (1993) 574.

[10] V. Barger et al. hep-ph/9905474v2 (1999)

[11] S. Degl'Innocenti, W. Dziembowski, G. Fiorentini and B. Ricci, Astr. Phys. 7 (1997) 77.

[12] G. Fiorentini and B. Ricci, Proceeeding of the International Workshop "Neutrino Telescopes '99",M.B. Ceolin ed, Venice 1999, astro-ph/9905341.

[13] S.Basu, M. H. Pinsonneault and J. N. Bahcall, astro-ph/9909247, to appear on Ap. J. (2000).

[14] G.Fiorentini and B.Ricci, "Beyond the Standard Model: from theory to experiment", World Scientific, Singapore 1999, astro-ph/980118.

[15] N. Grevesse and A. Noels, in "Origin and Evolution of the Elements", eds. N. Prantzos, E. Vangion-Flam and M. Cassé , Cambridge University Press, Cambridge 1993.

[16] J.N. Bahcall, S. Basu and M.H. Pinsonneault, Phys. Lett. B. 433 (1998) 1. (BP98)

[17] V. Castellani, S. Degl'Innocenti, G. Fiorentini, M. Lissia and B. Ricci, Phy. Rep. 281 (1997) 309.

[18] F. Ciacio, S. Degl'Innocenti and B. Ricci, Astron. Astroph. Suppl. Ser. 123 (1997) 449.

[19] O. Richard, S. Vauclair, C. Charbonnel and W. A. Dziembowski, Astron. Astroph. 312 (1996) 1000.

[20] G. Dvali and A. Y. Smirnov, hep-ph/9904211 (1999)

[21] G.S. Da Costa and T.E. Armandroff, Astron. J. 100 (1990) 162

[22] M. Salaris and. S. Cassisi, Monthly Not. Royal Astron. Soc. 298 (1998) 166

[23] V. Castellani, S. Degl'Innocenti and V. Luridiana, Astron. Astroph. 272 (1993) 442

[24] J.A. Frogel, J.G. Cohen, S.E. Persson, Ap. J. 275 (1983) 773

[25] F.R. Ferraro, P. Montegriffo, L. Origlia and F. Fusi Pecci, ESO preprint N. 1355, December 1999.

TABLES

TABLE I. Physical and chemical properties of the solar center, according to the SSM of [16].

T[K]	$1.569 \cdot 10^7$
ρ [g/cm^3]	152
X	0.33867
Y	0.64014
$\Sigma_j \frac{X_j}{A_j} Z_j^2$	1.06

TABLE II. KK-energy loss and production rates calculated at the solar center (see Appendix for definitions). Rates are in erg/g/s and the $4+n$ dimensional Planck mass M_s is in TeV/c^2.

	$n=2$	$n=3$
ϵ_γ	$2.75 \cdot 10^{-3} M_s^{-4}$	$2.63 \cdot 10^{-12} M_s^{-5}$
ϵ_{GB}	$1.59 \cdot 10^{-4} M_s^{-4}$	$8.26 \cdot 10^{-13} M_s^{-5}$
ϵ_{GCP}	$8.82 \cdot 10^{-4} M_s^{-4}$	$2.29 \cdot 10^{-12} M_s^{-5}$
ϵ_{KK}	$3.79 \cdot 10^{-3} M_s^{-4}$	$5.75 \cdot 10^{-12} M_s^{-5}$
ϵ_{ppI}	10.5	10.5

TABLE III. Fractional differences, (model-SSM)/SSM, between the calculated properties of a solar model with $M_s = 0.2$ TeV/c^2 ($n=2$) and the SSM.

initial composition	
Y_{in}	-2.3%
Z_{in}	+0.88%
convective envelope	
Y_{ph}	-2.5%
R_b	+0.08%
T_b	-0.72%
solar center	
X_c	-5.6%
Y_c	+3.0%
T_c	+1.7%
neutrino fluxes	
Be	+24%
B	+52%

TABLE IV. The best fit parameters for Eq. 6.

	$m[\mathrm{GeV/c^2}]$	α
$u_{0.2}$	60	4.3
Y_{ph}	80	4.1

FIGURES

FIG. 1. Fractional variation with respect to the SSM prediction, (model-SSM)/SSM, of the squared isothermal sound speed $u(r) = P/\rho$ in the solar model with $M_s = 0.2$ TeV/c^2 and $n = 2$. The shaded area corresponds to the "1σ" or statistical helioseismic uncertainty, see [6].

FIG. 2. Energy losses due to KK-graviton production along the solar structure of the model with $M_s = 0.2$ TeV/c^2 and $n = 2$. Dashed line corresponds to the photon-photon annihilation, dash-dotted line to gravi-Compton-Primakoff effects, dotted line to gravi-bremsstrahlung process. For a comparison also the nuclear energy production (full line) is shown.

FIG. 3. Fractional variation with respect to the SSM predictions of the quantities Y_{ph} (diamonds) and $u_{0.2}$ (squares) in the solar models with different values of M_s.

FIG. 4. The photospheric helium abundance Y_{ph} and the value of $u = P/\rho$ at $R = 0.2R_\odot$: a) as constrained by helioseismology, see Eqs. (5,4); b) as modified by models with the indicated value of M_s, in TeV/c^2).

FIG. 5. Upper panel: typical observational Hertzprung-Russel diagram for a galactic GC. Lower panel: the corresponding theoretical Hertzprung-Russel diagram. The most relevant evolutionary phases are shown.

FIG. 6. Time behaviour of the central temperature – density relation for a solar model from the Main sequence to the ignition of central He burning as predicted by present evolutionary calculations for the canonical case (std) and for the labelled values of M_s and $n = 2$.

FIG. 7. The mass, in solar units, of the He core at the central He ignition (RGB tip) as a function of M_s for n=2. In order to cover the range of metallicity (Z) spanned by the galactic GCs, computations have been performed for a $0.8M_\odot$ star with Z=0.0002 and for $1M_\odot$ star with Z=0.02.

FIG. 8. Luminosity (in bolometric absolute magnitudes) of the brightest observed RGB star (RGB tip) in clusters with different metallicities ([M/H] = Log(M/H)$_{\rm star}$ - Log(M/H)$_\odot$, where M is fractional abundance by mass of all the elements heavier than Helium) [24,25] as compared with theoretical predictions for the canonical scenario (std) and for models with energy losses due to KK-gravitons with the labelled values of M_s and $n = 2$.

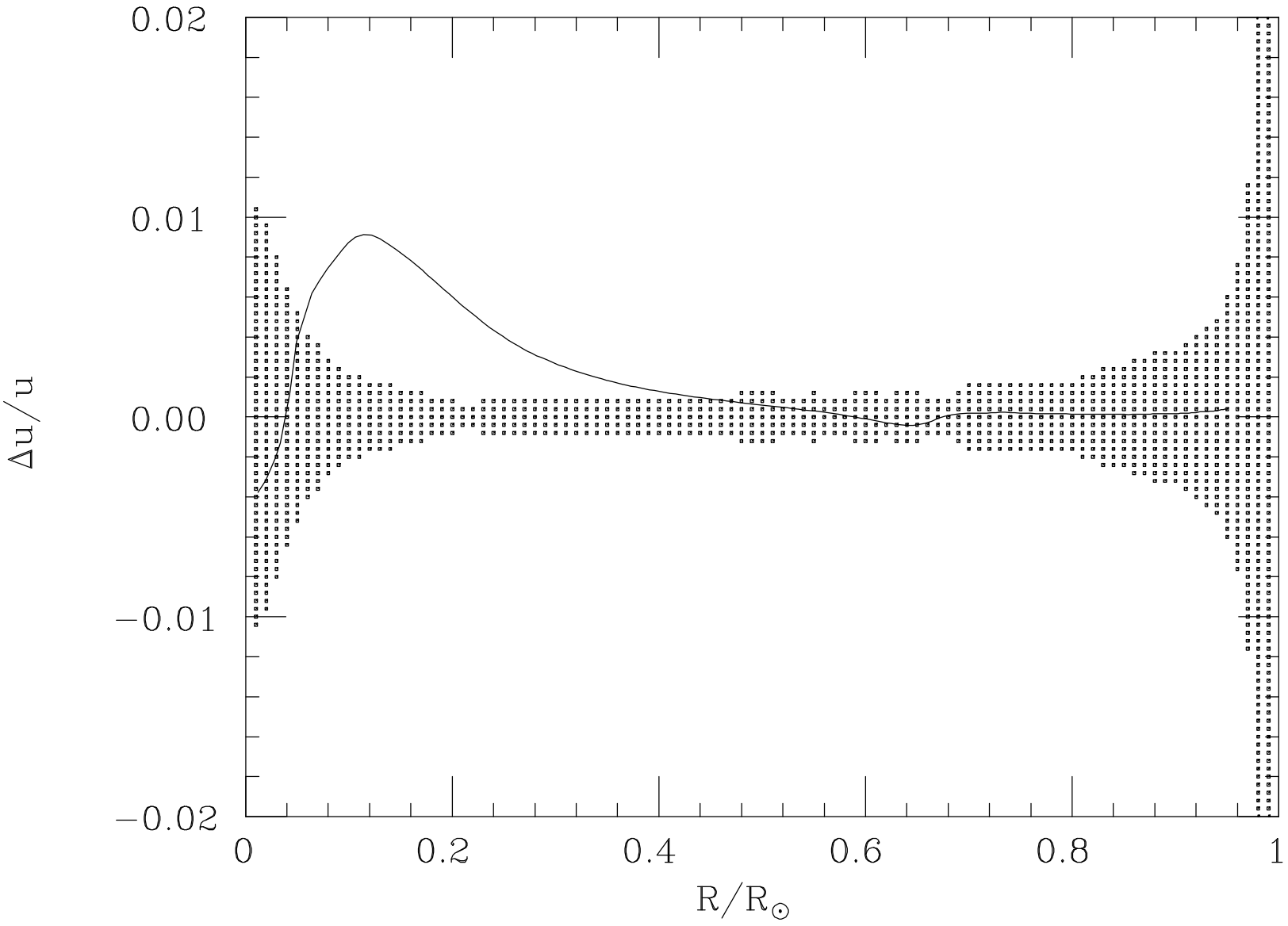

Fig. 1

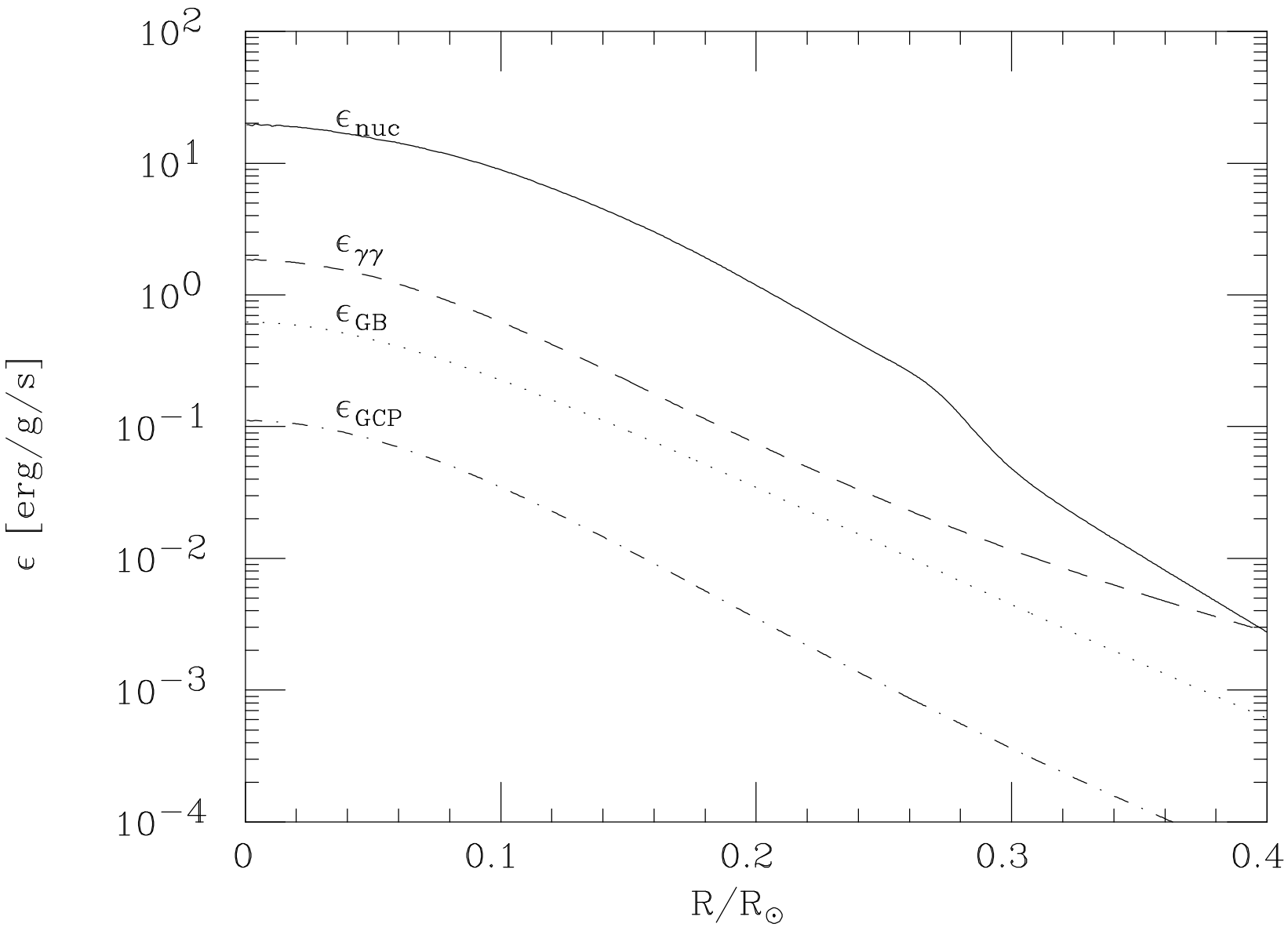
10^2
10^1
10^0
10^{-1}
10^{-2}
10^{-3}
10^{-4}
ϵ_{nuc}
$\epsilon_{\gamma\gamma}$
ϵ_{GB}
ϵ_{GCP}
ϵ [erg/g/s]
0
0.1
0.2
0.3
0.4
$R/R_\odot$

Fig. 2

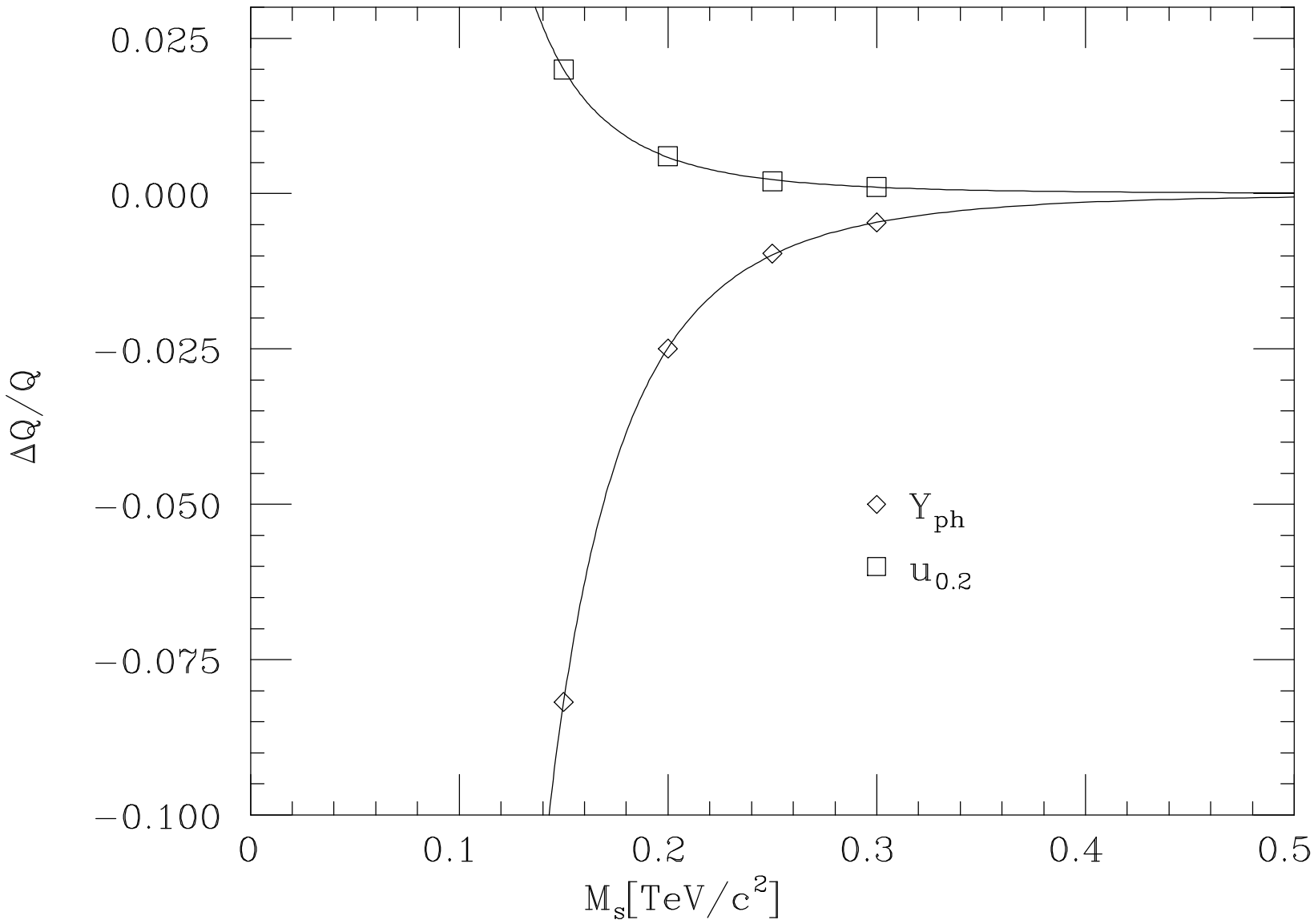
0.025
0.000
−0.025
−0.050
−0.075
−0.100
ΔQ/Q
0
0.1
0.2
0.3
0.4
0.5
M_s[TeV/c^2]
Y_ph
u_0.2

Fig. 3

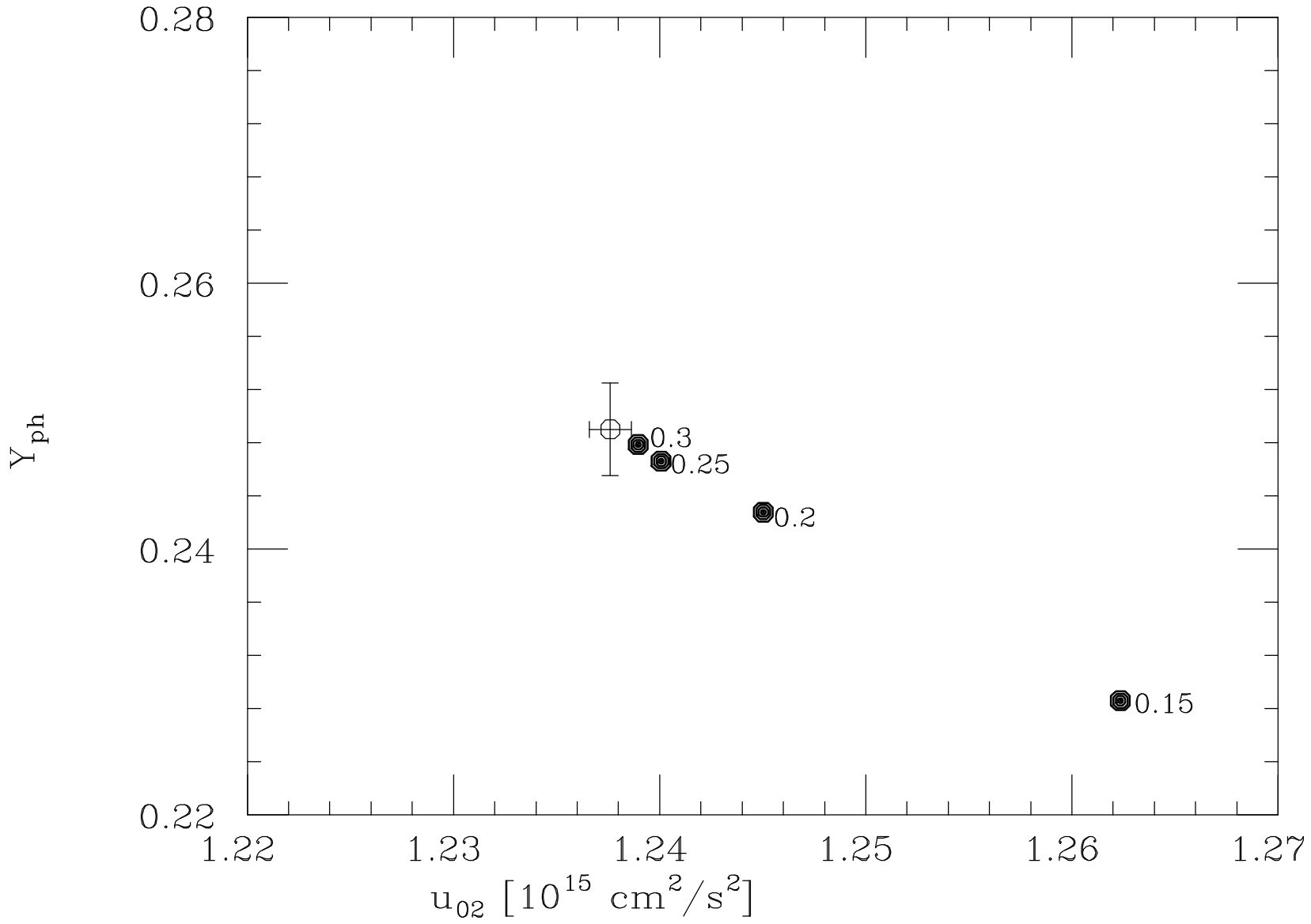
0.28
0.26
0.24
0.22
Y_{ph}
0.3
0.25
0.2
0.15
1.22
1.23
1.24
1.25
1.26
1.27
u_{02} [10^{15} cm^2/s^2]

Fig. 4

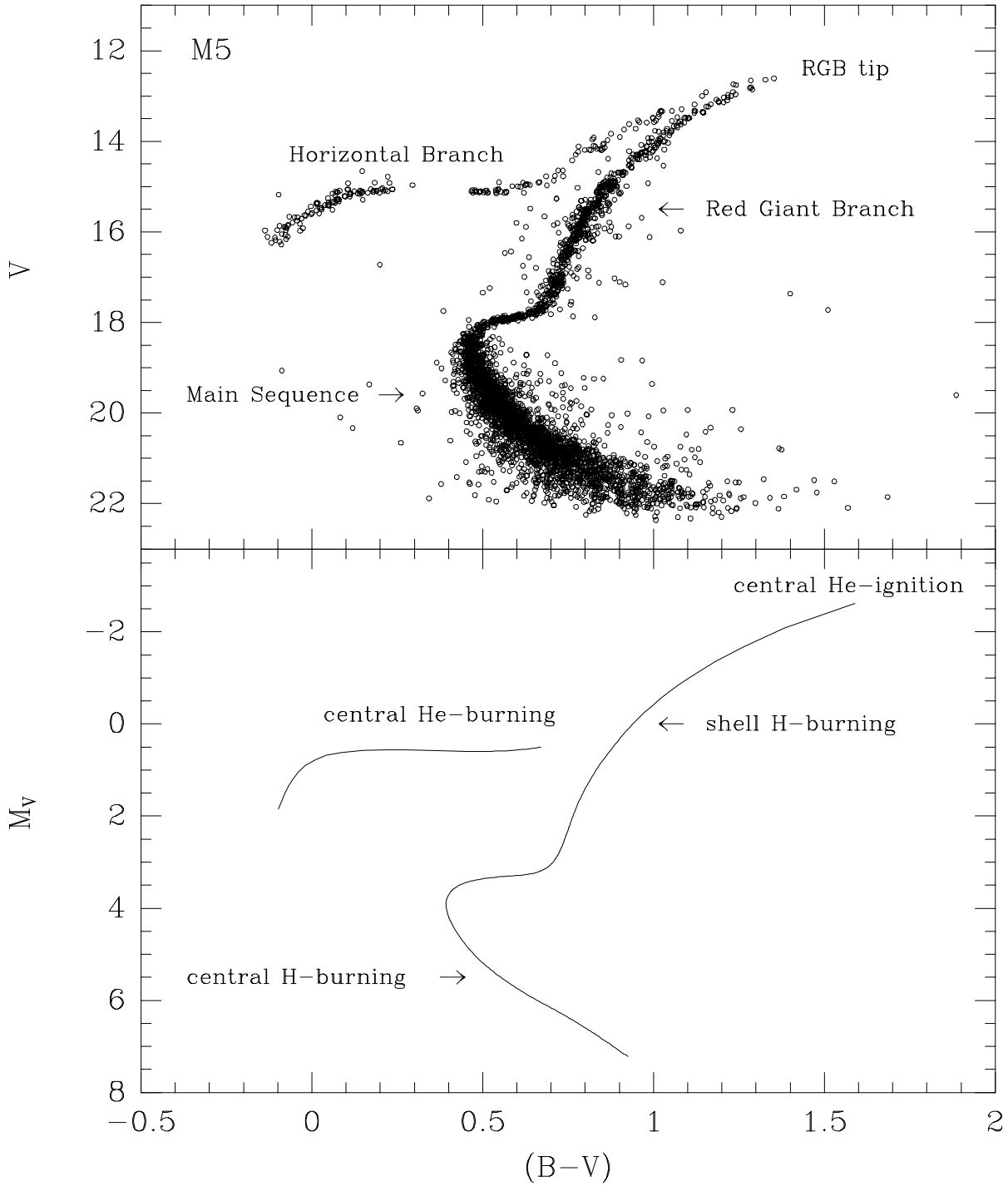
M5
RGB tip
Horizontal Branch
Red Giant Branch
Main Sequence
V
12
14
16
18
20
22
central He−ignition
central He−burning
shell H−burning
central H−burning
M_V
−2
0
2
4
6
8
−0.5
0
0.5
1
1.5
2
(B−V)

Fig. 5

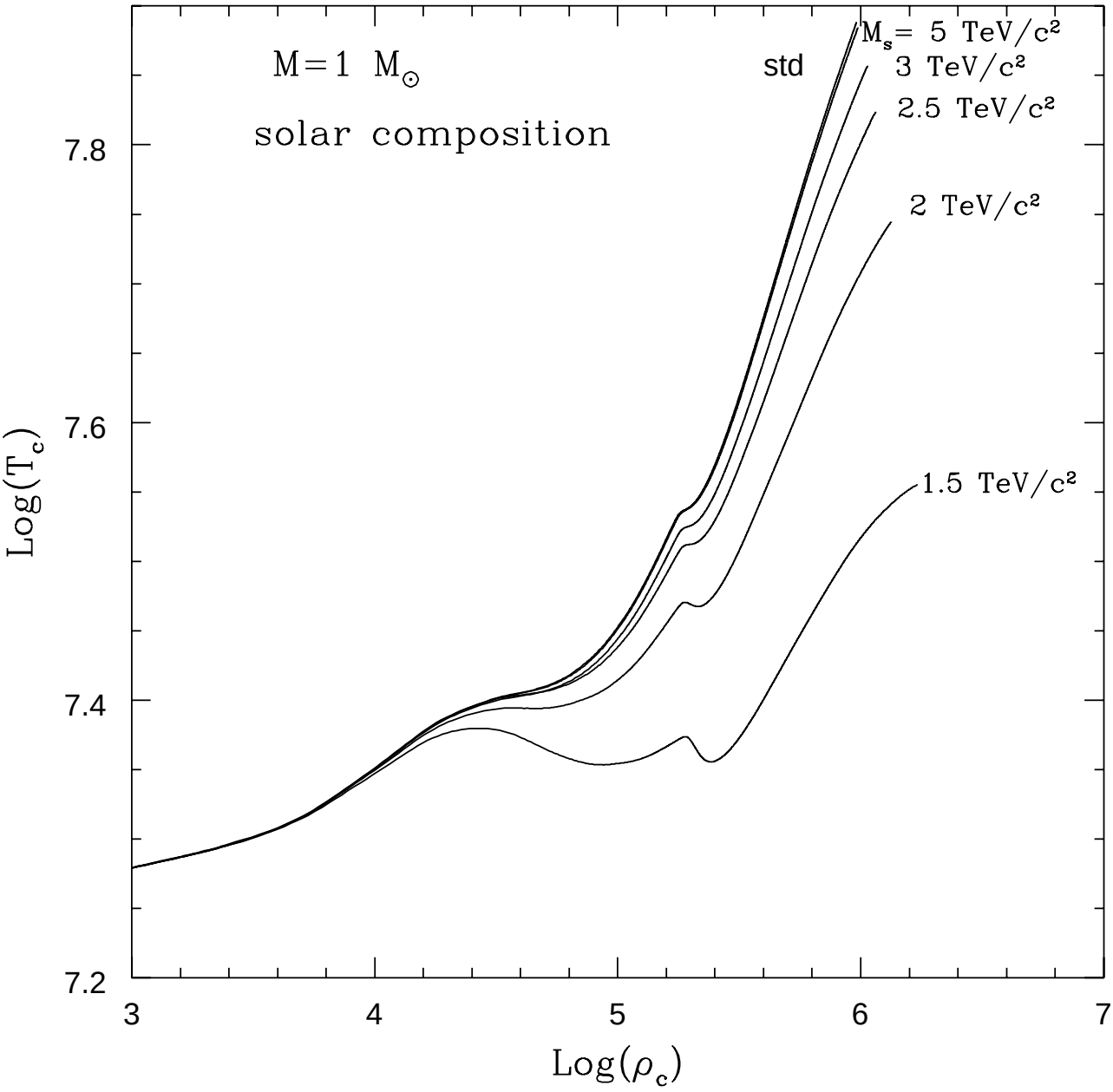
M=1 M⊙
solar composition
std
M_s= 5 TeV/c²
3 TeV/c²
2.5 TeV/c²
2 TeV/c²
1.5 TeV/c²
7.8
7.6
7.4
7.2
3
4
5
6
7
Log(T_c)
Log(ρ_c)

Fig.6

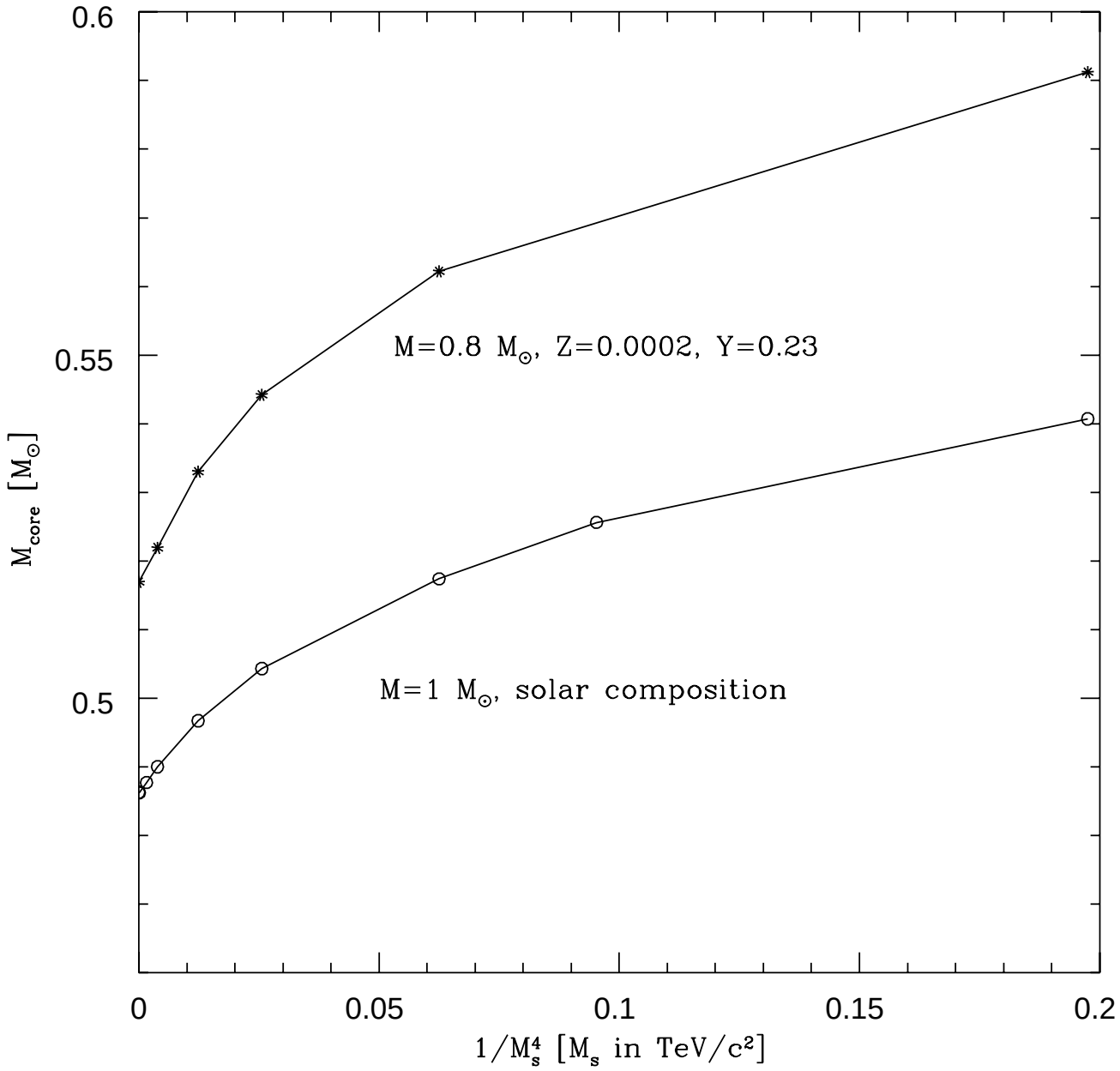
0.6
0.55
0.5
M_{core} [$M_\odot$]
M=0.8 $M_\odot$, Z=0.0002, Y=0.23
M=1 $M_\odot$, solar composition
0
0.05
0.1
0.15
0.2
$1/M_s^4$ [M_s in TeV/c^2]

Fig.7

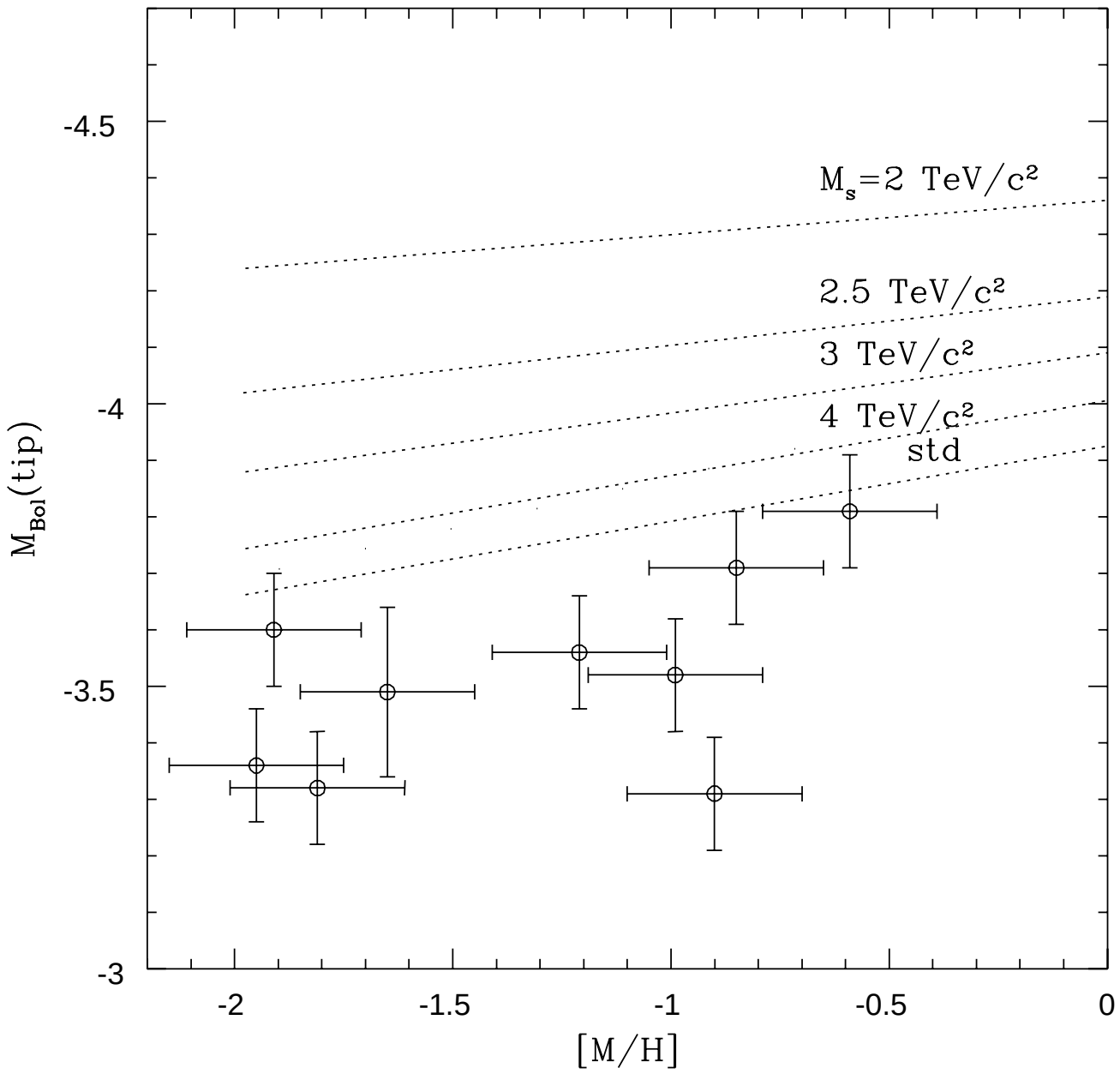
-4.5
-4
-3.5
-3
M_{Bol}(tip)
-2
-1.5
-1
-0.5
0
[M/H]
M_s=2 TeV/c²
2.5 TeV/c²
3 TeV/c²
4 TeV/c²
std

Fig.8